Cloning and Functional Analysis of a Rice NLR Immune Receptor Pair-RPR (Rice Paired Receptor) 1&2

Submitted by Fanlu Meng, to the University of Exeter as a dissertation for the degree of *Masters by Research* in Biological Sciences, January 2018.

I certify that all material in this dissertation which is not my own work has been identified and that no material has previously been submitted and approved for the award of a degree by this or any other University.

(Signature) …… Fanlu Meng ……

Cloning and functional analysis of a Rice NLR Immune receptor pair-RPR (Rice Paired Receptor) 1&2

Abstract

The intracellular nucleotide-binding leucine-rich repeat (NLR) immune receptors of plants often work in pairs to percieve pathogen effectors and innitiate immunity reponses. In this article, we focused on gene cloning and functional analysis of NLR paired protein RPR1 and RPR2 from *Oryza sativa Japonica*. This pair of NLR , which was obtained through bioinformatic analysis, shared high similairy with the previously reported pair of RPS4/RRS1 from *Arabidopsis*. Both RPR1 and RPR2 consisted Coiled-Coil domain at the N- terminal, while WRKY domains only appeared at the C- terminal of RPR2. By using Golden Gate cloning strategy, constructs of RPR1 and RPR2 for Level -1, Level 0, Level 1 were obtained. The subcellular localization pattern of RPR1&2 was analyzed by doing transient expression, and confocal imaging result indicated that this NLR pair localized within cell nucleus. RPR1 and RPR2 functioned together to recognize effector PopP2, which triggered HR- like response of chlorosis symptoms shown within co-infiltrated region.

Key words: Plant Immunity, NLR pair, Hypersensitive Reaction, Golden Gate Cloning

1. Introduction

To perceive and ward off pathogenic intruders, both plants and animals have developed the innate immune system, which is initiated via either cell surface (Pattern Recognition Receptors - PRRs) or intracellular receptors (Nucleotide binding domain (NBD) and Leucine-rich Repeat - NLRs) (Fig.1.1). The intracellular NLRs receptors recognize pathogen secreted virulence components, known as “effector” proteins, to active ETI (Effector Triggered Immunity), protecting multicellular organisms from microbial infection (Boller and Felix, 2009; Dodds and Rathjen, 2010; Elinav et al., 2011; Jones and Dangl, 2006). Plant and animal NLRs share considerable similarity with modular architecture, which consists of a N-terminal domain, a nucleotide binding domain (NBD) and a LRR (leucine-rich repeats) domain after NBD, while some kind of NLRs have C-terminal accessory domains (Duxbury et al., 2016; Jacob et al., 2013; Jones et al., 2016).

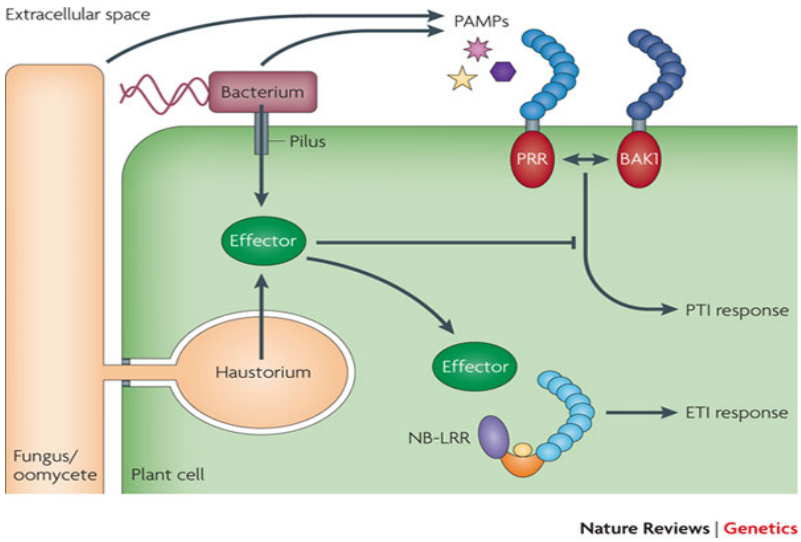

Figure 1.1. **The principles of plant immunity**. Molecules such as lipopolysaccharides, flagellin and chitin (pathogen- associated molecular patterns (PAMPs))，are recognized by cell surface pattern recognition receptors (PRRs) and elicit PAMP-triggered immunity (PTI). Bacterial pathogens deliver effector proteins into the host cell by a type-III secretion pilus, whereas fungi and oomycetes deliver effectors from haustoria or other intracellular structures by an unknown mechanism. These intracellular effectors often act to suppress PTI. However, many are recognized by intracellular nucleotide-binding (NB)-LRR receptors, which induces effector- triggered immunity (ETI). NB-LRR proteins consist of a carboxyl-terminal LRR domain (light blue), a central NB domain (orange crescent) that binds ATP or ADP (yellow oval), and an amino-terminal Toll, interleukin-1 receptor, resistance protein (TIR) or coiled-coil (CC) domain (purple oval). Dodds, P.N., and Rathjen, J.P. (2010). Plant immunity: towards an integrated view of plant-pathogen interactions. Nat. Rev. Genet. 11, 539–548.

Despite structural similarities, distinctions between plant and animal NLRs on domain architecture and functional mechanism are still obvious. It has been proposed that plant and animal NLRs likely evolved from distinct ancestral NBD lineages based on differential expansion from a common ancestor STAND AAA^{+} ATPases (Jones et al., 2016; Leipe et al., 2004; Yue et al., 2012) (Fig. 1.2). Plant NLRs use a subtype of STAND NBD called the NB-ARC (nucleotide-binding, Apaf1, Resistance, CED4) (Ea and Jones, 1998), while Animal NLRs carry a distinct NBD subtype NACHT (NAIP, CIITA, HET-E, and TP1) (Koonin and Aravind, 2000). The NBD domain is functional associated with ATP hydrolysis, playing an important role in NLR inactive/ activated state equilibrium shift (Koonin and Aravind, 2002; Yue et al., 2012). The N-terminal structure varies, but mainly falls in Coiled-Coil (CC) or Toll/Interleukin-1 Receptor (TIR) domains in plant NLRs, or the death-fold superfamily (such as CARD or Pyrin domains) in animal NLRs (Jacob et al., 2013). N-terminal domain is crucial for defense signal transduction by recruiting NLR oligomerizaiton accompanied with NBD-driven ATP hydrolysis, mechanism of which has already been testified in animals but not yet demonstrated in plants (Danot et al., 2009). Once signaling transduction activated, NLRs often induce a characteristic cell death response termed the "Hypersensitive Response" (HR) in plants and "pyroptosis" in animals. LRR domain seems negatively regulate NLR oligomerization through intermolecular/intramolecular NLR interaction (Hu et al., 2013; Duxbury et al., 2016). C-terminal domains are not always present in most NLRs, but are recruited as integrated decoy domain in some NLRs, for example the C-terminal CARD of NLRP1 in human (Chavarríasmith and Vance, 2013; Finger et al., 2012), and the WRKY transcription factor domain of RRS1 in *Arabidopsis* (Williams et al., 2014; Sarris et al., 2015; Le Roux et al., 2015).

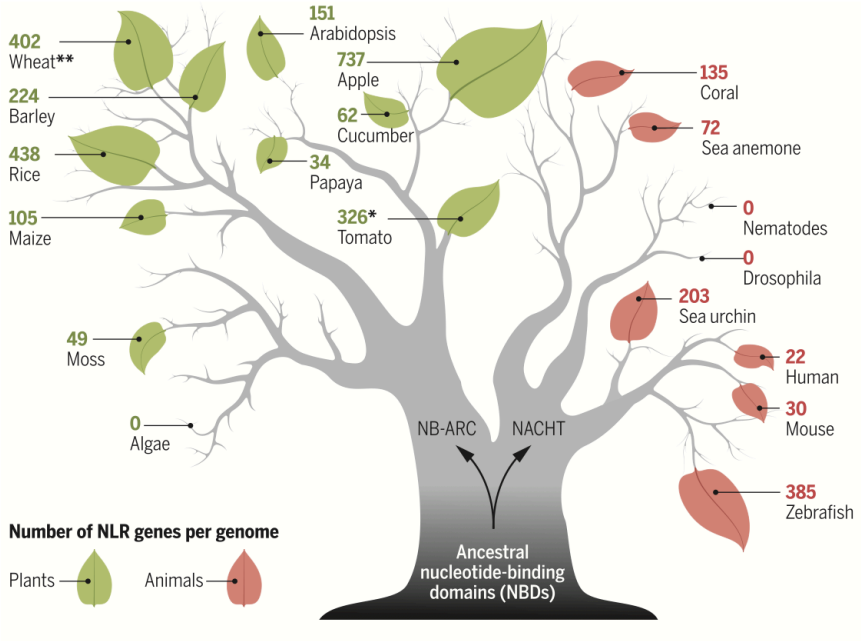

Figure 1.2. **NLR Tree.** Evolution of NLR genes followed diverging pathways for plant and animal species. NLRs likely derived from a common ancestor that expressed both NACHT and NB-ARC type NBDs. NACHT is found in animal NLRs, and NB-ARC in plant NLRs. Both occur in fungi. A variety of N- and C-terminal domains have been evolutionarily recruited onto NBDs, including those characteristic of NLRs. Jones, J.D.G., Vance, R.E., and Dangl, J.L. (2016). Intracellular innate immune surveillance devices in plants and animals. Science 354, aaf6395.

To discern the mechanism of NLR- effector recognition has recently been a rapid advancing and promising field that contribute to articulate ETI activation process. Many NLRs can sense effectors by direct interaction. For example, the TNL (TIR-NB-ARC-LRR) RPP1 of *Arabidopsis* can directly recognize effector ATR1 from *Hyaloperonospora Arabidopsidis* (Schreiber et al., 2016). However, the “gene-to-gene” based direct recognition model cannot explain everything. Alternatively, the “**guard model**” or the “**decoy model**” which include the “host protein” within the recognition process have been proposed. For example, the host factor RIN4 targeted by effector AvrRpm1 under the surveillance of NLR RPM1 in *Arabidopsis* just fits the “guard model” (Mackey et al., 2002), while the tomato NLR Prf monitors effector-targeted protein kinases of the Pto family is considered as the “decoy model” (Ntoukakis et al., 2014) (Fig. 1.3). The decoy factor can also be recruited within NLRs as an integrated domain, such as the integrated decoy-WRKY of NLR RRS1 (Sarris et al., 2015; Le Roux et al., 2015) and HMA of RGA5 (Césari et al., 2014).

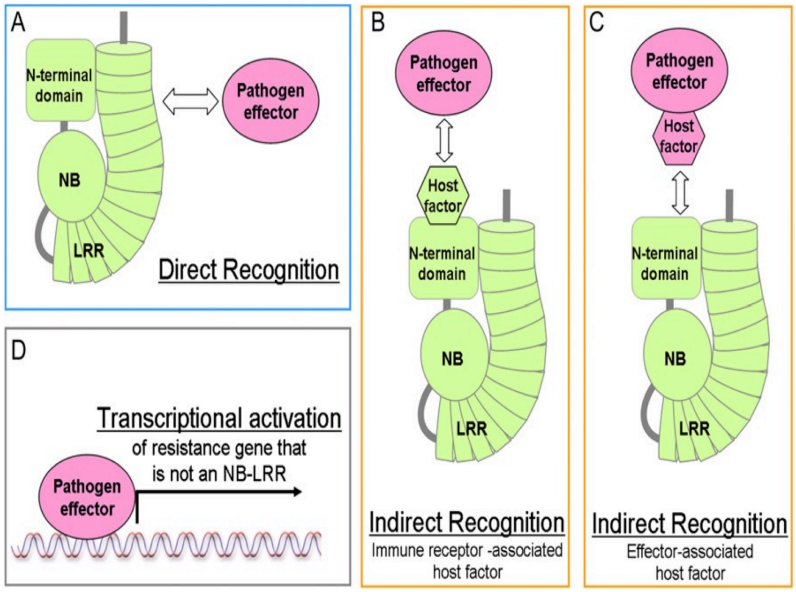

Figure 1.3. **The Three Modes of Pathogen Recognition.** (A) Pathogen recognition can occur if NB-LRR immune receptors (green) directly bind pathogen effectors (pink). Alternatively, NB-LRRs can indirectly recognize pathogens through the N-terminal domain (CC or TIR) using an intermediary host factor. The host factor (also referred to as guardee) can be constitutively associated with the immune receptor (B) or it may first associate with the pathogen effector (C) and then is subsequently recognized by the immune receptor. The third type of recognition occurs when a pathogen effector mimics a transcription factor and directly induces the expression of a non-NB-LRR resis- tance protein (D). Jeffrey Caplan, *et al,* 2008. Plant NB-LRR Immune Receptors: From Recognition to Transcriptional Reprogramming, Cell Host & Microbe.

Recent studies suggest that the integrated decoy model can be applied in paired NLRs, of which one with the fusion domain bind the effector, whereas the other (the “helper NLR”) is required for its downstream signaling (Saucet et al., 2015; Kroj et al., 2016; Sarris et al., 2016). *Arabidopsis* paired TNLs RPS4 and RRS1 are linked proteins that can perceive two unrelated bacterial type III effectors (T3E), the YopJ family acetyltransferase PopP2 (Tasset et al., 2010) and the *P. syringae*pv. *Pisi* AvrRps4 effector (Gassmann et al., 1999). The C-terminal sequence of RRS1 is an “integrated decoy” WRKY-domain, which stands for a transcription factor family, with a conserved WRKYGQK motif followed by a $C_{x4–5}C_{x22–23}H_xH$ or $C_{x7}C_{x23}H_xC$ zinc-finger motif (Chi et al., 2013; Williams et al., 2014; Sarris et al., 2015). WRKY proteins are implicated in defense, and the effector targets as well in *Arabidopsis*. In case of the paired NLR proteins RPS4/RRS1, effectors can be trapped by RRS1 through WRKY domain and convert the RPS4/RRS1 complex into activation state, initiating defense responses (Sarris et al., 2015; Le Roux et al., 2015) (Fig. 1.4).

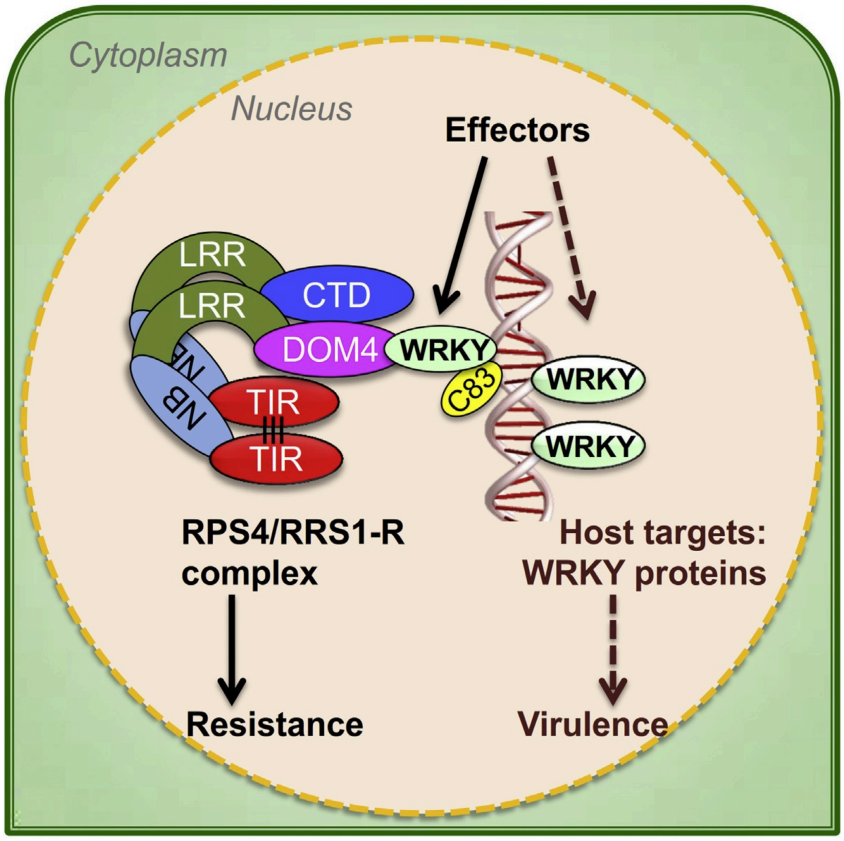

Figure 1.4. **The schematic diagram of the paired NLRs RPS4/ RRS1 working model.** An *Arabidopsis* intracellular immune receptor complex, one component of which contains A WRKY DNA binding domain, detects specific bacterial effectors to activate defense. Acetylation of WRKY domains by an effector likely interferes with host defense and this domain in the receptor complex enables detection of pathogen effectors that broadly target WRKY domain proteins. Panagiotis F. Sarris *et al,* May 21, 2015. A Plant Immune Receptor Detects Pathogen Effectors that Target WRKY Transcription Factors. Cell 161, 1089–1100.

This discovery shed lights on elucidating the co-evolutionary process of host-microbe interaction. WRKY itself is the target of effector in host plants. Interestingly, plants take advantage of that by integrating WRKY as an ID (Integrated Decoy-domain), within the C-terminal of the NLR protein, trapping effectors that target WRKY transcription factors. Plants turn weakness into strength, and it seems that plants evolved to take this strategy during long-term resisting pathogens. Interestingly, AvrRps4 and PopP2 are unrelated effector from different bacteria, and they can interact with WRKY through different mode of action. It seems that NLR- ID may convergent different effectors stimulus into the same pathway, providing the potential explanation for effector diversity is connected to the limited key host cell targets. Interestingly, previous study demonstrated that interfamily transfer of paired RPS4/ RRS1 genes confers resistance to multiple pathogens (Narusaka et al., 2013), indicating the discovery

of linked paired NLRs in plants may help functional transfer of plant NLRs across taxonomical barriers, enhancing prospects for crop disease control through genetic breeding.

Integration of protein domain into NLR receptors, has been found widespread across different plant taxa, and recent studies of genome-wide analyses have led to mining novel IDs and NLR proteins (Bonardi et al., 2012; Cesari et al., 2014; Sarris et al., 2016). The newly discovered domains fused to NLRs, in various plant genomes, provide a new perspective on effectors targets and the nature of pathogenicity, as well as, the host susceptibility. Integrated domains and effector targets overlap, to some extant, providing multiple levels of information encoded in NLR-IDs (Fig. 1.5). In terms of the overlap between the predicted NLR fused domains and the effector targets, IDs could be used to validate pathogen-derived virulence factors and identify new sources of disease resistance. Besides, NLR-IDs investigation will undoubtedly enrich our knowledge of the co-evolutionary history of host and pathogens, leading to new ways of engineering disease resistance (Sarris et al., 2016).

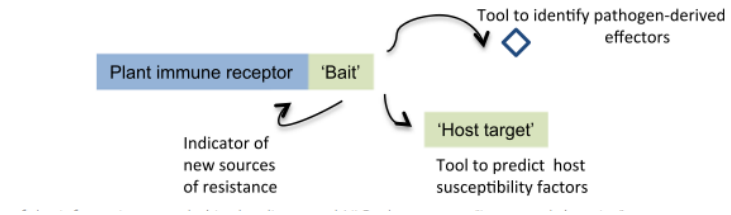

Figure 1.5. **Summary of the information encoded in the discovered NLRs that possess "Integrated domains".** Overlap between fusions and effector targets point to the multiple levels of information encoded in NLR-IDs. Presented NLR-IDs are likely to be molecular sensors of the effectors, so they can also be exploited to identify and validate pathogen-derived virulence factors. For many pathogens, researchers have now accumulated long lists of predicted effector molecules that are likely to be secreted or translocated inside plant cells. Systematic analyses of these effectors against the NLR-IDs in either proteomic or yeast two-hybrid assays would allow for prioritization and validation of pathogen effectors. These validation tools represent an important milestone for deciphering pathogen arsenals and identifying new sources of disease resistance. Sarris *et al,*2016. Comparative analysis of plant immune receptor architectures uncovers host proteins likely targeted by pathogens. BMC biology 14, 8.

In this MSc thesis, the paired proteins RPR1& 2 (Rice Paired Receptor 1 & 2) are a set of hypothetical CC-NLRs (CNLs) discovered though genome analysis in *Oryza sativa Japonica*. The work plan is to PCR amplify and clone the genomic DNA of RPR1& 2 genes individually, using the Golden Gate modular cloning strategy, and to perform a primary functional analyses

by exploiting Golden Gate constructs via transient expression in *Nicotiana tabacum* (tobacco) plants (Fig. 1.6).

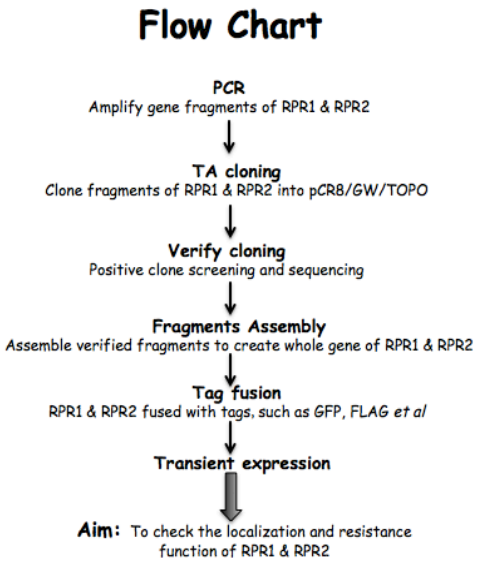

Figure 1.6. **The work flow chart of the RPR1& 2 project.** Fanlu Meng.

The rice originated RPR1 & 2 have shared high sequence similarity with RPS4/RRS1 from *Arabidopsis*. As a result of that, our work maintains the potential to deduce the demonstrated paired NLR-decoy model from *Arabidopsis* (*Brassicaceae*) to rice (*Gramineae*), providing profound effects on cross-taxon resistance research. *Oryza sativa* is commonly known as Asian rice that plays a crucial role in the global food security, which is a critical issue especially in the developing world. About 3 billion people, nearly half the world's population, depend on rice for survival. In Asia as a whole, much of the population consumes rice in every meal. In many countries, rice accounts for more than 70% of human caloric intake (http://www.bios.net/daisy/RiceGenome/3649/3591.html). Our research work will pose far-reaching impact on addressing important disease issues of rice.

2. Materials and Methods

2.1 Plant Materials and Growth Conditions

Nicotiana benthamiana (Nb) and *Nicotiana tabacum* (Nt) plants were grown in long days (16 hr light/8 hr dark) at 24°C.

2.2 Primer design and Polymerase Chain Reaction (PCR) amplification of DNA fragments

The Golden Gate cloning system is based on Type IIs restriction Endonuclease that enables the digestion and ligation working at the same time- “one pot, one step”. Type IIs restriction enzymes are able to cleave DNA outside of their recognition site, resulting in 5’ or 3’DNA overhangs (depending on the enzyme) that can consist of any nucleotide. Therefore, 256 different overhangs can be created using a type IIs restriction endonuclease that produces a 4 nt overhang, giving great flexibilities to the primer and construct design (Engler et al., 2009; Engler et al., 2008; Engler et al., 2014; Weber et al., 2011). *BsaI* and *BpiI* are the enzymes commonly used for Golden Gate system. All the *BsaI* or *BpiI* enzyme restriction sites should be eliminated from the target gene sequence through fragment PCR of Level -1, and then the gene fragments are assembled to create the whole gene in Level 0. The standard Level 0 parts, such as promoter, 5’-UTR, signaling peptide, CDS gene sequence, tag, 3’- UTR, terminator, etc., are recruited in order to get the Level 1 construct. Level 2 allows different gene units express at the same time (Fig. 2.1).

Figure 2.1. **Golden Gate MoClo Assembly Standard.** Standard (level zero) parts are assembled from single or multiple sequences either directly or via intermediate level −1 fragments. Level zero parts are assembled into level one acceptor backbones to make complete transcriptional units. Multigene constructs can be made by assembling level one constructs in level 2, M, or P acceptor backbones. Engler C. *et al*, 2009. A golden gate modular cloning toolbox for plants. ACS synthetic biology 3, 839-843.

Primer design is crucial for Golden Gate cloning. The gene sequence of RPR1 has 8011bp with a *BsaI* site at 251bp; for RPR2, the sequence length is 3541bp with a *BsaI* site at 2927bp. Gene sequences are divided into several parts (RPR1 is divided into 6 compartments, and RPR2 into

3 compartments, Fig. 2.2) and eliminated the inner *BsaI* site through primer design. The genomic fragments of RPR1 (6 fragments) and RPR2 (3 fragments) were amplified with primers containing 4bp specific overhangs and *BsaI* recognition sequence.

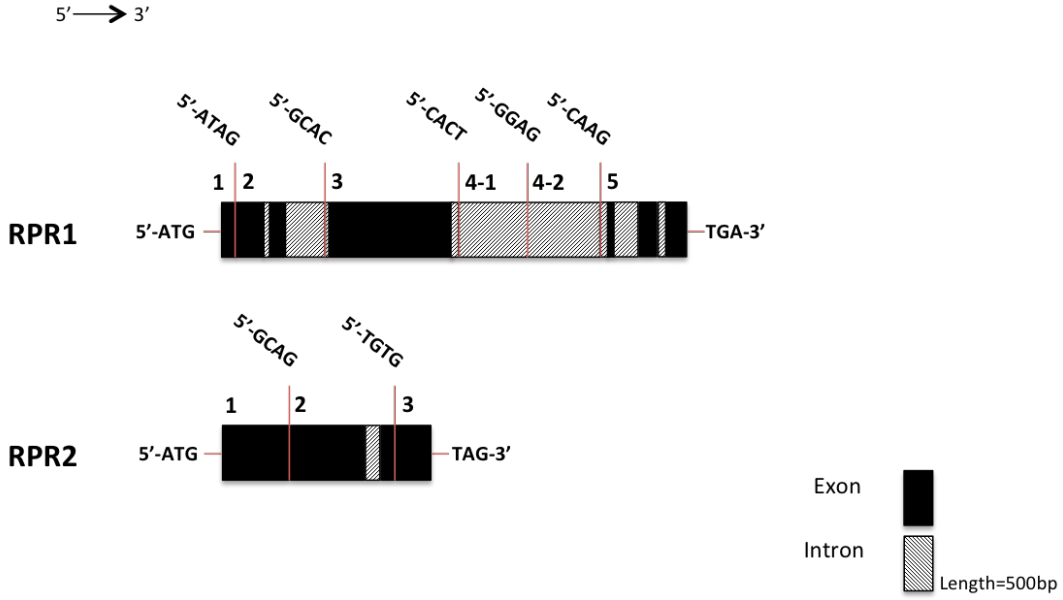

Fig. 2.2. **Genomic DNA segmentation of RPR1 and RPR2.** The black represents exon, and strip represents intron. RPR1 is separated into 6 parts- 1, 2, 3, 4-1, 4-2, 5, while RPR2 is separated into 3 parts- 1, 2, 3. The 4bp specific overhangs of each part are marked out. Fanlu.

Phusion High-Fidelity DNA Polymerase (NEB, M0530) was used to carry out the PCR experiments by following procedures as the manual described. Annealing temperature used in Phusion PCR was roughly 5°C higher than the mean Tm value of the primer pairs.

2.3 Agarose gel electrophoresis and purification

The concentrations of agarose gels used are from 0.8% to 2.5%, depending on the size of bands needed to be separated. TAE buffer was applied in both gel docking and running. Briefly, agarose powder was weighed and mixed with proper volume of 1xTAE, heated to completely dissolved. Once cooling down to about 50°C, add ethidium bromide (EtBr) to a final concentration of approximately 0.2-0.5 μg/mL. Pour the agarose into a gel tray with the well comb in place, carefully avoiding air bubbles. Once solidified, the agarose gel was placed into the gel tank filled with 1xTAE buffer, subjected to electrophoresis at 80~120 V for 30~50 minutes with DNA ladder and samples loaded.

To extract the desired DNA band from gel, Gel and PCR Clean-Up System (Promega A9280)

was used to carry out the gel purification procedures by following the kit instructions. DNA eluted from the SV Mini column were quantified and stored at -20°C.

2.4 A-tailing and T-A cloning

T-vector pCRTM8/GW/TOPO (Invitrogen K2500-20) was chosen as golden gate Level -1 vector to accept the purified PCR fragments, for the reason that it doesn't carry any *BsaI* site. As Phusion PCR created blunt ends, A-tailing was performed to add adenine to the 3'- end before connected to T vectors. 10μl A-tailing reactions system, which was consisted of 4μl purified DNA fragments, 1 μl 10X Taq DNA polymerase buffer, 2 μl dATP (1mM), 1 μl Nuclease-free water, and 1μlDNA polymerase, were set up on ice and incubated at 72°C for 30 minutes. This reaction was terminated by ice cooling and stored in -20°C freezer. 4 μl A-tailing Product was subjected to do T-A cloning through mixed and incubated with 1 μl Salt Solution and 1 μl TOPO vector at room temperature (22–23°C) for 5 minutes. The mixture was proceeded to transform One Shot Competent *E. coli* (kit provided) by using the freeze-thaw protocol. The resulting transformation was evenly spread on LB agar plate containing *Spectinomycin* antibiotic, and incubated overnight at 37°C. Colonies were picked and cultivated for analysis.

2.5 Plasmid Isolation

Both Alkaline Lysis method (manual protocol) and Promega Miniprep kit were used to isolate plasmid DNA. For alkaline Lysis method, bacteria harvested from 5 mL culture was re-suspended in Solution I (50 mM glucose, 10 mM EDTA, 25 mM Tris, pH 8.0. Stored at 0℃) and vortex as necessary for fully re-suspension. 250 μl room temperature (RT) solution II (freshly prepared 0.2 N NaOH, 1% SDS) was applied into mixture to lysis the bacteria followed by repeated gentle inversion. 200 μl ice-cold Solution III (3M KOAc, pH 6.0) was subsequently added to the lysate, and gently inverted several times. The mixture was subjected to centrifugation and isopropanol precipitation. After washed with ice-cold 70% ethanol, the DNA pellet was dissolved in 30~40 μl ddH_2O. RNA was eliminated by addition of 1 μl RNase A (10mg/ml) and incubation for 20 minutes RT.

Minipreps DNA Purification System (Promega, A1330) was applied to isolate plasmid with high purity for sequencing and stock. All the experiment procedures were performed as the kit instruction described. Purified DNA were stored at -20°C or below.

2.6 Enzyme digestion for construct screen

To screen positive cloning, enzyme digestion method, which should be more sensitive and reliable compared to colony PCR, was adopted. The restriction enzyme sites within the construct were analyzed and aligned one by one. Suitable restriction enzymes were chosen first to form the hypothetical restriction graphs. Digestions were then put on by using the enzymes selected and analyzed by electrophoresis. Positive cloning was screened by comparing the gel to the hypothetical digestion pattern.

2.7 Plasmid construction- Level 0 and Level 1 of Golden Gate cloning

At firstly, all the plasmid DNA should be adjusted to the equal module number of copies, about 2.0~ 3.0 x 10^{10} copies/ µl. Vector backbone, equimolar amounts of the other assembly pieces and reagents were mixed on ice to reach a total volume of 15µl. Detailed recipes were as below:

Table 2.1. Recipe for Golden Gate digestion

components	**Volume**
All DNA Plasmids	1µl of each
10X NEB T4 DNA ligase Buffer	1.5µl
BSA (10mg/ ml)	1.5µl
BsaI- HF	1µl
NEB T4 DNA ligase	1µl
ddH20	Add to reach to a total volume of 15µl

Mixture was subjected to a thermocycler as below:

Table 2.2. Golden Gate Thermocycler

Step	**Temperature**	**Time**
25 cyles	37°C	3 minutes
	16°C	4 minutes
1 Cycle	50°C	5 minutes
	80°C	5 minutes

Use 5 µl of the assembly reaction mix to transform 100 µl of electrocompetent *E. coli*.

2.8 Preparation of electrocompetent cells and electroporation

To prepare electrocompetent cells, *E.coli* DH5α single colony was cultivated in SOB medium (2% tryptone, 0.5% yeast extract, 10 mM NaCl, 2.5 mM KCl ,10 mM $MgCl_2$, 10 mM, $MgSO_4$) to reach an OD600 of 0.5-0.7. Bacteria was spun down and re-suspended in 10% pre-chilled glycerol. It was then washed twice by repeated centrifugation and re-suspension. Bacteria was finally suspended in 10% glycerol by pipetting up and down (1L initial culture was finial suspended in 5 mL 10% glycerol), and allocated in 1.5mL Eppendorf tubes- 50ul/tube. The electrocompetent cells could be directly subjected to electroporation or stored in a -80°C freezer. 1mm electroporation cuvettes and LB plates with appropriate antibiotic were pre-chilled on ice before electroporation. DNA ready for transformation was mixed with electrocompetent cells gently and thoroughly. Apply DNA-cell mixture on cold cuvette and press pulse to start electroporation. Immediately add 950 µl of 37°C SOC (SOB medium with addition of 20 mM glucose), and recover bacteria in the 37°C incubator. 100 µl bacteria was plated on pre-warmed plate with appropriate antibiotics.

2.9 Blue white selection

Blue white selection was applied to screen positive cloning at the Golden Gate Level1 stage, because vector pISL86922 carries blue/white selection marker. Briefly, 7 µl IPTG (0.1 mM) and 20µl X-gal (40 mg/mL) was applied on the top of pre-made agar petri dish and spread evenly with a hockey stick spreader. Once dry, bacteria was plated on the top.

2.10 Preparation of Agrobacterium competent cells and Agroinfiltration

Agrobacterium competent cells was prepared by using calcium chloride method. Culture was started from a single colony of freshly streaked *Agrobacteria* strain Agl1, and pre-chilled before centrifugation (low speed 4,000 rpm at 4°C.). Once spun down, bacteria were re-suspended by adding ice cold 20 mM calcium chloride (50ml initial culture was re-suspended in 5ml 20 mM calcium chloride). The suspension was spun down and washed again with 20 mM calcium. At last, the 50ml initial culture was re-suspended in 2.5 ml 20 mM calcium, and allocated in 2 ml Eppendorf tube for 200 µl/tube. Freeze-thaw method was applied to transform *Agrobacteria* competent cells. 500ng DNA was added into 1 tube *Agrobacteria* competent cells, and kept on ice for 30 minutes. The tube was then shifted to liquid nitrogen for 5 min, and subjected to heat shock in 37°C water bath for 5 min, then returned to ice for 5 minutes. 1 ml of LB medium was added to the bacteria, which was then incubated on a 28°C rotating shaker for 3 hours. 100 ul of culture was spread on the top of a LB plate containing antibiotics of *Rifamycin*, *Kanamycin*

and *Carbenicillin*. Plates would stay at 28°C for 2 d and proceeded to colony PCR to confirm transformation.

For agroinfiltration in *N. benthamiana* (confocal microscopy) and *N. tabacum* (HR induction), *Agrobacterium tumefaciens* strains AgI1 were transformed with various binary constructs. *Agrobacterium* strains carrying different constructs were grown in liquid LB-medium supplemented with adequate antibiotic for 24 hours. Cells were harvested by centrifugation, washed in 5ml of 10 mM $MgCl_2$ and re-suspended infiltration medium (10 mM $MgCl_2$, 10 mM MES pH 5.6). For *Agrobacteria* carrying RPR1 and RPR2 constructs, adjust OD600 to 0.4, while use OD600 = 0.25 for effector constructs. For co-expression, bacterial suspensions were mixed in 1:1 ratio before infiltration with 1ml needleless syringe in 4-5week-old*N. benthamiana* or *N. tabacum* leaves. Tobacco programed cell death was generally observed and photographed 2-3 days after infiltration.

2.11 Confocal microscopy imaging

Infiltrated leaves were visualized with confocal microscopy (Zesis LSM 510META, Germany) using 40×/1.2 W C-Apochromat or 63×/1.4 Oil Plan-Apochromat in multi-track channel mode. Excitation wavelengths and emission filters were 488 nm/bandpass505-530 nm for YFP, 458 nm/band-pass 465-530 nm for CFP, and 488 nm/band-pass 650-710 nm for chloroplast auto-fluorescence. The images are presented as 3D projected stacks of neighboring sections. Image processing was performed using LSM 510 version 4.2 (Zeiss).

2.12 RNA extraction and Reverse Transcription

To amplify CDS DNA fragment of RPR1 and RPR2, mRNA should be extracted and reverse transcripted. Qiagen RNeasy kit was used to extract total RNA from agro-infiltrated *N. benthamiana* leaves by following the kit protocol. Briefly, about 100 mg leave tissue was frozen in liquid nitrogen, grinded thoroughly, and re-suspended in 450 µl Buffer RLT by vigorous vortex. Lysate was transferred to a QIA shredder spin column (lilac) placed in a 2 ml collection tube, and centrifuged for 2 min at full speed. The supernatant of the flow-through was transferred to a 1.5ml Eppendorf tube, and mixed with 0.5 volume of ethanol (96–100%) by immediate pipetting. The sample was applied on an RNeasy spin column (pink) placed in a 2 ml collection tube, followed by a centrifugation for 15 s at ≥8000 x g (≥10,000 rpm). Buffer RW1 and 500 µl Buffer RPE were successively added to the column and spun down to wash the column membrane. RNA was eluted from the column and dissolved in 50 µl RNase-free water.

RNA extracted with high purity was subjected to synthesis of first-strand cDNA Using Agilent cDNA synthesis kit. The master mix was 20 µl, including 10 µl of first strand master mix (2×), 3 µl of oligo (dT) primer (0.1 µg/ µl), 1.0 µl of Affinity Script RT/ RNase Block enzyme mixture, 4 µl of extracted RNA (~700ng/ µl) and 2 µl RNase-free H2O.

3. Results

3.1 Sequence analysis

The paired proteins RPR1& 2 (Rice Paired Receptor 1 & 2) are a set of hypothetical CC-NLRs (CNLs) discovered though genome analysis in *Oryza sativa Japonica*. The RPR1 & 2 pair shares high sequence similarity with RPS4/RRS1 which is a pair of NLRs from *Arabidopsis* (Fig. 3.1). Similar to RRS1, RPR1 also carries WRKY domain at the C-terminal. The difference is that there is only one WRKY within RRS1 but are two in RPR1, giving more possibilities to this research work. Another difference of the rice pair concerns the N-terminal part of these receptors. Unlikely to the RPS4/RRS1 pair, which are TIR-NLRs (TNLs), the N-terminal region of RPR1 & 2 is CC (Coiled-Coil) domain, which maintains high similarity with The *potato virus X* resistance (RX) protein. As a typical CNL protein that confers resistance against *Potato Virus X*, RX protein shows a nucleocytoplasmic localization, and both nuclear and cytoplasmic pools are required for full defense activation. The N-terminal coiled-coil domain of RX has been shown to interact with RanGAP2, which is a necessary co-factor in the resistance response (Conserved Protein Domain Family, NCBI) (Hao et al., 2013; Rairdan et al., 2008).

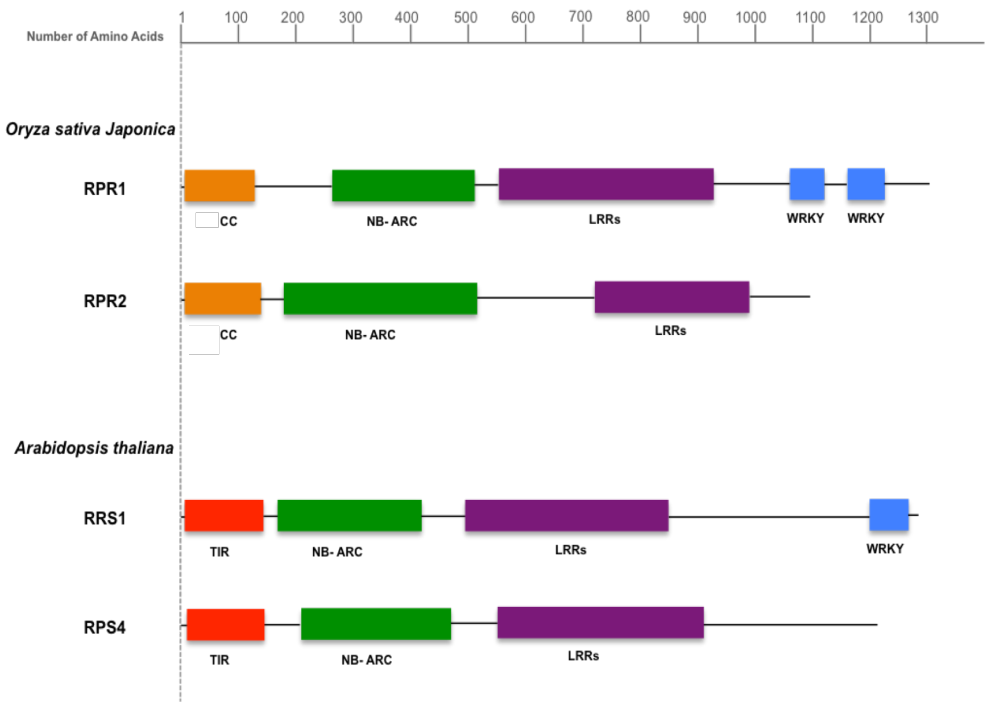

Figure 3.1. **Structural comparison of RPR1& 2 from *Oryza sativa* and RPS4/RRS1 from *Arabidopsis*.** The scale bar on top stands for the number of Amino Acids. The domain structures of RPR1& 2 (*Oryza sativa Japonica*) and RPS4/RRS1 (*Arabidopsis thaliana*) were compared and exhibited within this map, in which green colour boxes represent NB-ARC domain, purple colour boxes represent LRRs domain, blue colour boxes represent WRKY domain, orange colour boxes represent CC domain, and red colour boxes represent TIR domain.

3.2 DNA fragment amplification and T-A cloning

DNA fragments were amplified by fusion PCR. Primers designed for PCR contained 4bp specific overhangs and *BsaI* enzyme digestion site (List of primer). The RPR1-Fragment1 with the length of 253bp was amplified at the annealing temperature of 65°C, RPR1-Fragment2 1527bp annealing at 65°C, RPR1-Fragment3 2330bp annealing at 68°C, RPR1-Fragment4-1 1228bp annealing at 56°C, RPR1-fragment4-2 1280bp annealing at 56°C, RPR1-Fragment5 1438bp 65°C (Figure S1 A, B). RPR2 was cut into 3 fragment, with RPR2- Fragment1 1163bp, RPR2- Fragment2 1770bp and RPR2- Fragment3 608bp (Figure S1 C). 1µl DNA ladder and 1µl of each DNA sample were loaded onto each gel. Cleaned PCR products were subjected to do T-A cloning. The transformation plates after T-A cloning of RPR2- Fragment1,2,3, was shown (Figure S1 D), while for RPR1 the transformation result was omitted as the plates looked rather alike.

For the gene cloning we used the Golden Gate cloning system (Engler et al., 2009; Engler et al., 2008; Engler et al., 2014). Restriction endonuclease *EcoRI* was used to screen the T-A cloning, which was for the Golden Gate cloning level -1. Take RPR1-fragment 1 for example: hypothesis *EcoRI* digestion maps for empty T vector pCRTM8/GW/TOPO and RPR1-fragment 1 integrated T vector had shown different restriction patterns, with only one band (2799bp) for empty vector and two bands (2799bp and 293bp) for the T vector integrated with RPR1-fragment 1. The physical nucleic gel on the right hand side exhibited the digestion results, with positive cloning screened out marked with red arrow (Figure S2 A). For RPR1-fragment 2, there were three bands, 2799bp, 1440bp, and a short band of 127bp which is too dim to see on the gel (Figure S2 B). For RPR1-fragment 5, there were two bands with the length of 2799bp and 1467bp, respectively (Figure S2 B). T-A cloning vector carrying with the RPR1-fragment 3 was split into two pieces, 2799bp and 2370bp, which were too close to be well separated on the gel. The gel at the bottom was the same with the one on the top, with just longer electrophoresis time and shorter exposure time. The red arrow marked on the gels indicates the positive cloning screened (Figure S2 C). Fragment 4-1 and 4-2 of RPR1 were as shown (Figure S2 D). Cloning of Fragment 4-1 was digested into 2 fragments, and 3 positive constructs were selected. Fragment 4-2 was cut into 4 bands with 4 positive constructs were screened. For RPR2, the T-A cloning screen was as shown (Figure S2 E), with red arrow marked the positive cloning on the gel. All the positive cloning screened by enzyme digestion method should be subjected for sequencing to ensure the DNA sequence accuracy.

3.3 Making Golden Gate level 0 construct pICSL01005::RPR2

Vector pICSL01005 was adopted to make level 0 construct. As pICSL01005 carried *Spectinomycin* antibiotic selection marker that was the same with T vector pCRTM8/GW/TOPO, it would create difficulties for level 0 cloning. For RPR2, we have successfully screened positive construct by using enzyme digestion method. pICSL01005::RPR2 was digested into two bands, 3907bp and 1881bp (Fig 3.2 A). Positive constructs were marked with red arrows (Fig 3.2 B). In terms of RPR1, we failed to get its level 0 construct, because 6 fragments were expected to be assembled and linked intopICSL01005, making it difficult to screen the re-assembly plasmid out of 7 kinds of input plasmids (the input plasmids included T vectorintegrated with each DNA fragment of RPR1, and vector pICSL01005). As a result of that, we skipped the Level 0 step, and proceeded to Golden Gate Level 1.

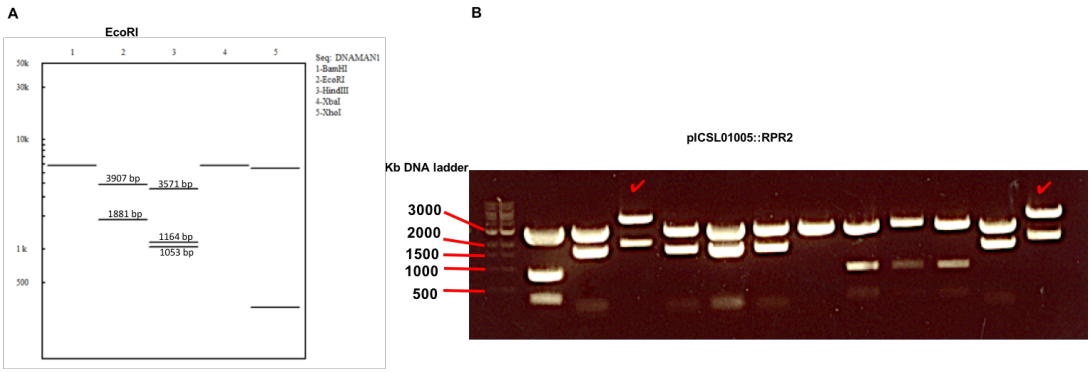

Figure 3.2. **Construct pICSL01005::RPR2 screen through enzyme digestion. (A)** Hypothetical *EcoRI* restriction graphs of pICSL01005::RPR2. *BamHI*, *EcoRI*, *HandIII*, *XbaI* and *XhoI* are applied to form the restriction map. Lane 2 shows that the pICSL01005::RPR2 could be theoretically digested by *EcoRI* into two bands: 3907bp and 1881bp. **(B)** Physical gel for *EcoRI* digestion screen of pICSL01005::RPR2. Two red arrows have marked out the positive constructs whose two-band digestion pattern is in accordance with the theoretical map (A).

3.4 Making Golden Gate level 1 construct

Vector pICSL86922 was chosen as the Golden Gate level 1 vector to accept NLR gene fused with corresponding tag. To make construct pICSL86922::RPR2-YFP, equal amount of pICSL01005::RPR2, pICSL50005 (carry YFP tag) and pICSL86922 (golden gate level 1 vector) were mixed then subjected to a golden gate thermocycler. Blue/ white selection was adopted after ligation and electroporation. The negative control plate, which stayed above with dozens of white and blue white colonies, was from the ligation with only pICSL50005 and pICSL86922 (Fig 3.3 A). The plate below with thousands of white colonies and several blues ones were from the ligation of pICSL01005::RPR2, pICSL50005 and pICSL86922 (Fig 3.3 A). White colonies from the plate below were picked, cultivated and screened through Mini-prep followed by an enzyme digestion. *EcoRI* digested pICSL86922::RPR2-YFP should create 3 bands: 7136bp, 2275bp and 1891bp, while *EcoRI* digestion of empty vectorpICSL86922 should also show 3 bands but with different size: 5955bp, 1891bp and 1668bp (Fig 3.3 B). It could tell from the gel that every cloning was positive (Fig 3.3 C).

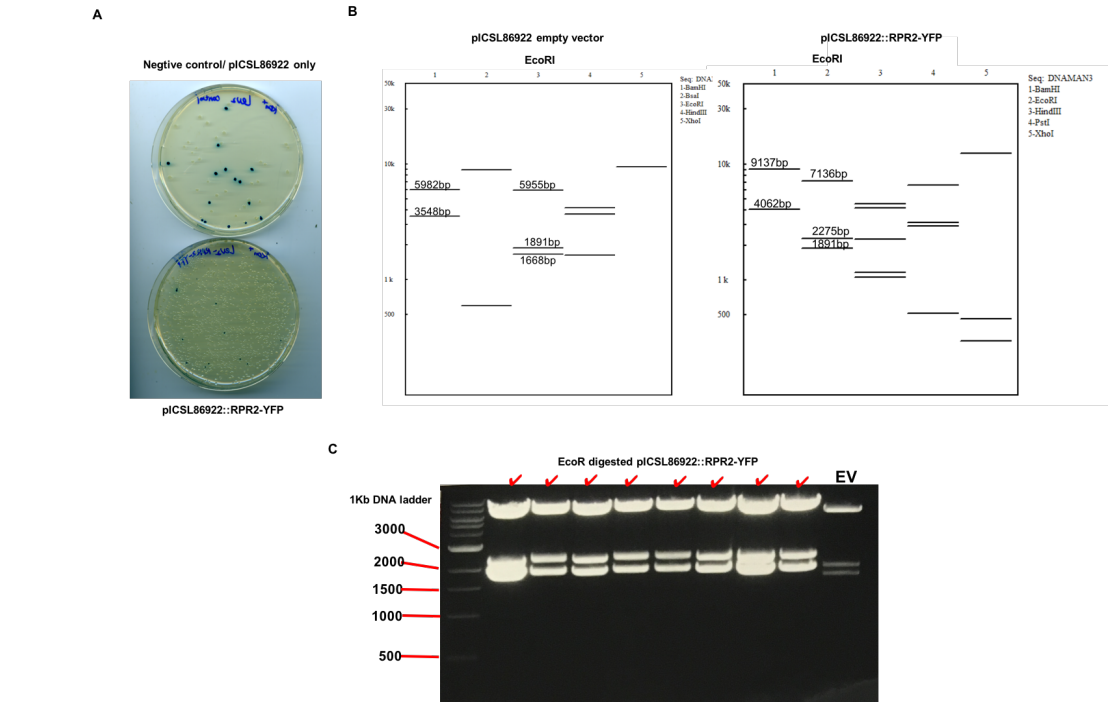

Figure 3.3. **Making Golden Gate Level 1 Construct pICSL86922::RPR2-YFP. (A)** Transformation plates for pICSL86922::RPR2-YFP. The petri dish on the top shows the negative control, which is from the ligation with only pICSL50005 and pICSL86922, while the plate below with far more colonies is from the ligation of pICSL01005::RPR2, pICSL50005 and pICSL86922. **(B)** Hypothetical *EcoRI* restriction graphs of pICSL86922::RPR2-YFP. The pictures show both pICSL86922 empty vector (left) and pICSL86922::RPR2-YFP (right) digestion patterns. Different enzymes (such as *EcoRI, HindIII, BamHI, XhoI, PstI, XbaI,* etc.) are applied to form the digestion graph, and the lane with *EcoRI* is marked out. **(C)** Physical gel for *EcoRI* digestion screen of pICSL86922::RPR2-YFP. All the sample lanes (marked with red arrows) show the same digestion pattern with the hypothesis map, and the EV lane stands for pICSL86922 empty vector digestion.

As mentioned before, Level 0 cloning of RPR1 was not obtained, so at this stage all the RPR1 fragments (Fragment1, 2, 3, 4-1, 4-2, 5) linked with T vector, pICSL50020 (carry eCFP tag) and pICSL86922 went to ligation, electroporation and blue/ white selection. The negative control with only blue colonies was for vector pICSL86922 only, while the two plates below with mainly white colonies were for pICSL86922::RPR1-eCFP but of different volume (200µl, 50µl) of culture spread on the top of Petri dishes (Fig 3.4 A). Hypothesis digestion graphs for pICSL86922 and pICSL86922::RPR1-eCFP were as shown (Fig 3.4 B). Restriction enzyme *BamHI* (Fig 3.4 C) and *EcoRI* (Fig 3.4 D) were both used to carry out the enzyme digestion. Positive cloning was marked with red arrow (Fig 3.4 E). To ensure this assembly, PCR was done by using the screened plasmid #1 and #6 as template and different primer pairs (Figures S1 B). It could tell from the gel that band size (Figures S3 A) were as expected (Figures S3 B).

The whole length of RPR1 genomic DNA was amplified by using plasmid as template and Frg1 Fw& Frg5Rv as primer set (Figures S3 C). Purified PCR product of RPR1 was inserted into vector pICSL01005, and screened by *EcoRI* enzyme digestion (Figures S3 D and E). Positive cloning was marked with red arrow.

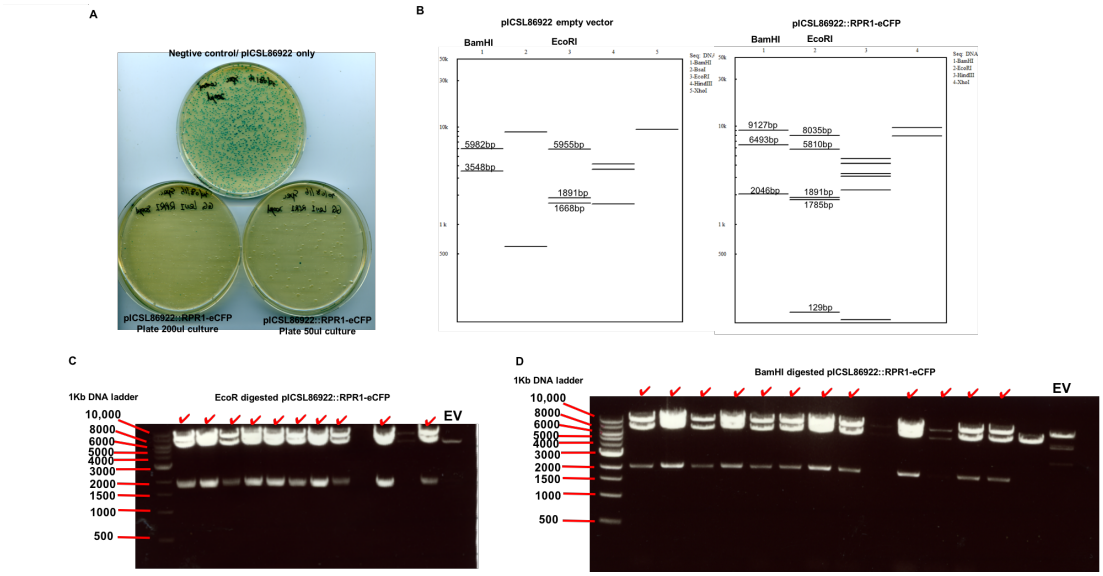

Figure 3.4. **Making Golden Gate Level 1 Construct pICSL86922::RPR1-eCFP. (A)** Transformation plates for pICSL86922::RPR1-eCFP. The top plate (show only blue colonies) is the negative control for ligation and transformation with vector pICSL86922 only, while the two petri dishes below with mainly white colonies are for pICSL86922::RPR1-eCFP with different volume (left size plate- 200µl , right side plate- 50µl) of culture spread. **(B)** Hypothetical *EcoRI* and *BamHI* restriction graphs of pICSL86922::RPR1-eCFP. The pictures show both pICSL86922 empty vector (left) and pICSL86922::RPR1-eCFP (right) digestion patterns. Different enzymes (such as *EcoRI, HindIII, BamHI, XhoI, PstI, XbaI,* etc.) are applied to form the digestion graphs, and the lanes with *EcoRI* and *BamHI* are marked out. **(C)** Physical gel for *EcoR*I digestion screen of pICSL86922::RPR1-eCFP. The sample lanes marked with red arrows show the same digestion pattern with the hypothesis map, and the EV lane stands for pICSL86922 empty vector digestion. **(D)** Physical gel for *BamHI* digestion screen of pICSL86922::RPR1-eCFP. The sample lanes marked with red arrows show the same digestion pattern with the hypothesis map, and the EV lane stands for pICSL86922 empty vector digestion.

In addition to pICSL86922::RPR1-eCFPand pICSL86922::RPR2-YFP, other level 1 constructs, such as pICSL86922::RPR1-YFP, pICSL86922::RPR2-mCherry and pICSL86922::RPR2-eCFP, were prepared in the same way (Figures S4).

3.5 RPR1 and RPR2 localized in the plant cell nucleus

In agroinfiltration assays in *N. benthamiana*, RPR1 fused to eCFP tag and RPR2 fused to YFP tag were expressed in injected leaf section and observed under confocal microscopy. Both

RPR1-eCFP (Fig 3.5 A, B) and RPR2-YFP localized in the plant cell nucleus (Fig 3.5 C, D). The expression control of all fusion proteins was controlled by the CaMV 35S promoter (35S).

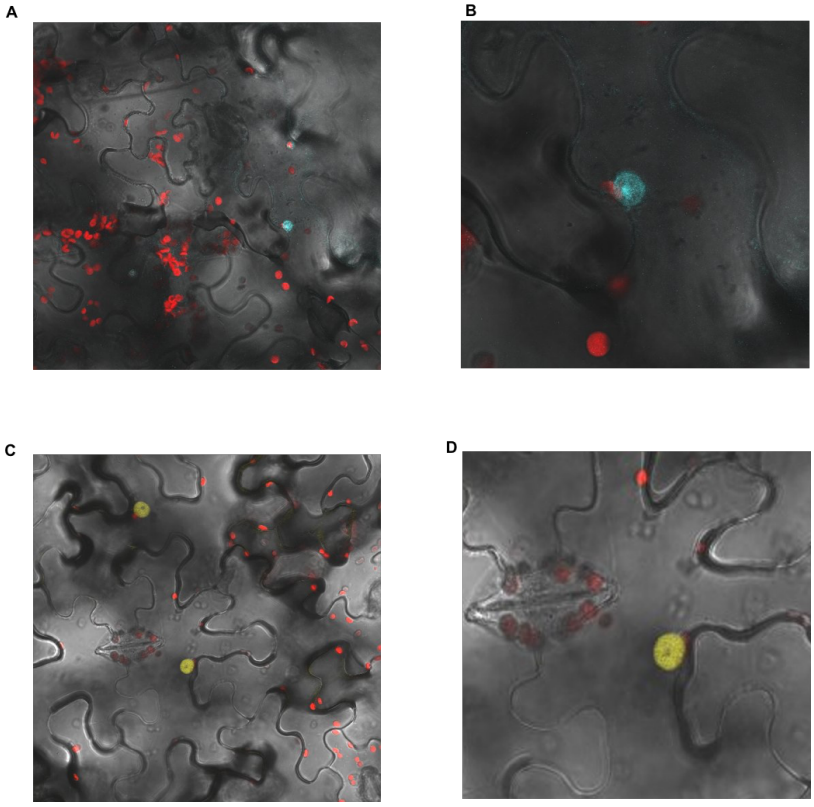

Figure 3.5. **Confocal imaging. (A)** Confocal imaging of RPR1- eCFP transient expression. The cyan colour indicates the RPR1-eCFP signal, while the red color stands for the autofluorescence of chloroplast. RPR1- eCFP accumulates within nucleus. **(B)** "Zoom in" view of (A). **(C)**Confocal imaging of RPR2- YFP transient expression. The yellow colour indicates the RPR2-YFP signal, while the red color stands for the autofluorescence of chloroplast. RPR2- YFP accumulates within nucleus. **(D)** "Zoom in" view of (C).

3.6 Early HR response was observed when effector PopP2 co-infiltrated with RPR1 and RPR2

We tested whether the effectors AvrRps4 or PopP2 were recognized by NLR pair RPR1/RPR2, by the activation of the Hypersensitive Response (HR). At the agroinfiltration assays in *N. tabacum*, leaf sections co-expressing the RPR1/RPR2 pair showed early HR-like response to PopP2. In contrast, leaf sections infiltrated with PopP2 only, or individually RPR1, RPR2 or both RPR1/RPR2 pair without the PopP2 effector, did not show the same yellow lesion symptoms (Fig 3.6, Figure S5). However, effector AvrRps4 didn't trigger HR response (Data not show), which indicates absence of specific recognition.

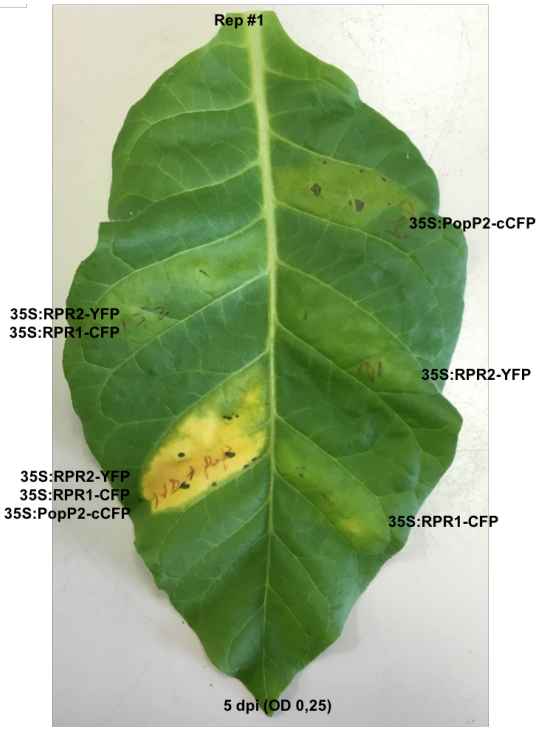

Figure 3.6. **HR test of paired cc-NLR RPR1&2 with effector PopP2.** At the agroinfiltration assays in *N. tabacum*, five treatments were carried out within one leaf: infiltrate with RPR1 only, RPR2 only, PopP2 only, co-infiltrate with RPR1/RPR2 pair, and co-infiltrate with effector PopP2 and RPR1/RPR2 pair. Only PopP2 and RPR1/RPR2 co-infiltration show yellow lesion symptoms.

3.7 Making the cDNA cloning of RPR1 and RPR2

N. tabacum leaf sections expressing gDNA of the RPR1 and RPR2 genes (35S::RPR1 and 35S::RPR2), were collected and subjected to total RNA extraction (Fig 3.7 A). RT-PCR was performed by using primer sets RPR1-Frg1 Fw& Frg5Rv (for RPR1 cDNA), and RPR2-Frg1 Fw&Frg3Rv (for RPR2 cDNA). Different annealing temperatures, ranging from 53.5°C to 59.5°C, were adopted in the RT-PCR. For RPR2, the expected cDNA size should be 3879bp, and the band was quite specific at 59.5°C (Fig 3.7 B). 3294bp should be the hypothesis size of RPR2 cDNA, and the biggest the band indicated with red arrow seemed to be the right size (Fig 3.7 B). The right size bands were harvested from gel, purified and linked to vector pICSL01005. Positive cloning was screened via enzyme digestion method. For RPR2, *HindIII* was used for the digestion (Fig 3.7 D). The positive cloning marked with red arrow took the majority (Fig 3.7 C). For pICSL01005::cDNA(RPR1), the transformation seemed not that efficient, because only several colonies came out (data not show). 3 colonies were picked and tested by *SacI* digestion and cDNA PCR. The No. 3 marked with red arrow should be the desired right cloning, as its *SacI* digestion (Fig 3.7 E) was in accordance to the hypothesis

digestion map (Fig 3.7 F), and the PCR band was identical to its whole length.

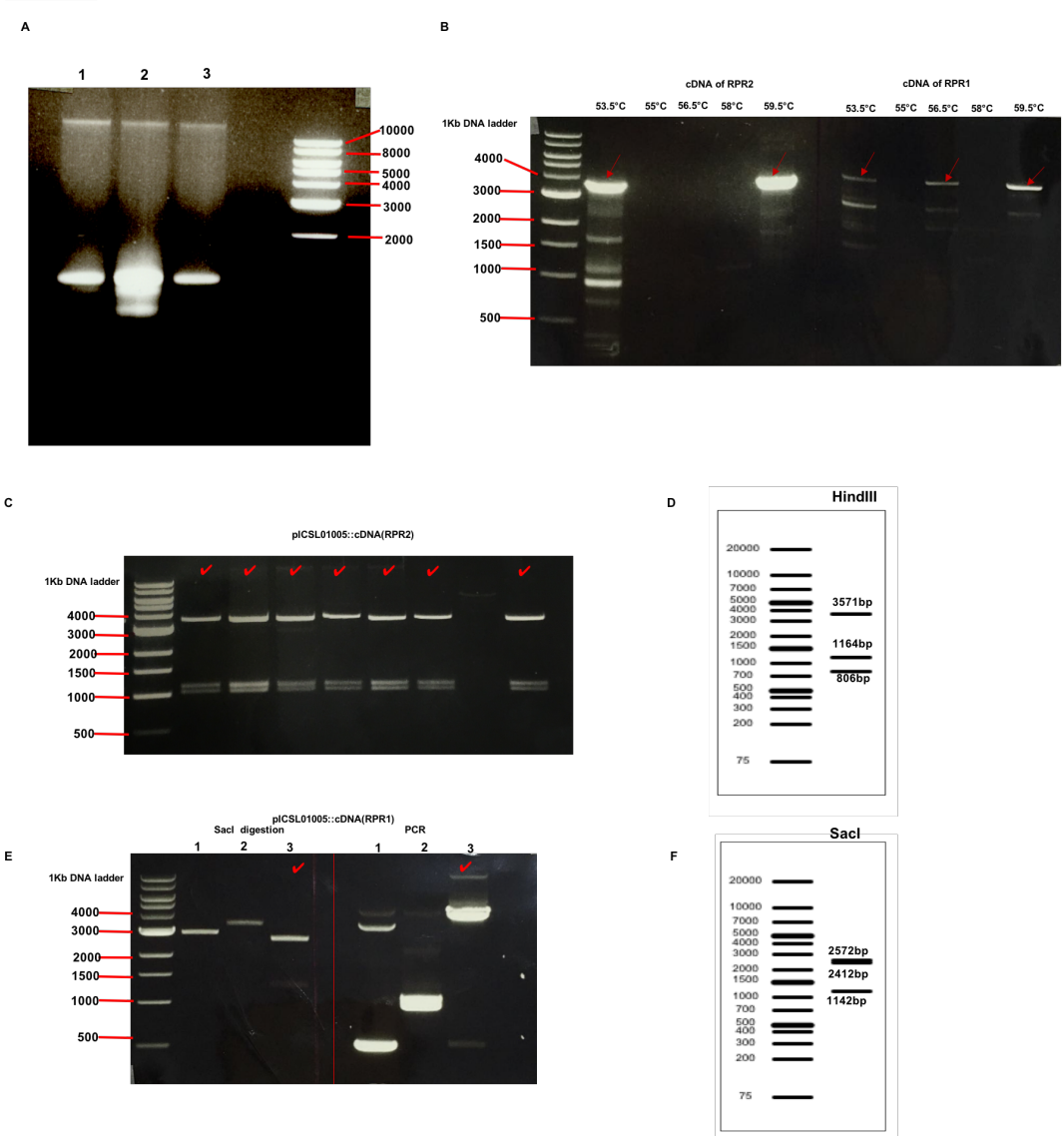

Figure 3.7. **cDNA cloning of RPR1 and RPR2. (A)** RNA extraction. From left to right show the RNA extraction from samples of RPR1 infiltration, RPR2 infiltration and RPR1&2 co-infiltration **(B)** cDNA PCR of RPR1 and RPR2. Annealing temperatures ranging from 53.5°C to 59.5°C, are adopted in the RT-PCR. For RPR2, the expected cDNA size should be 3879bp, and the band was quite specific at 59.5°. 3294bp should be the hypothesis size of RPR2 cDNA, and the biggest the band indicated with red arrow seemed to be the right size **(C)** Physical gel for *HindIII* digestion screen of pICSL01005::cDNA (RPR2). Red arrows have marked out the positive clonings whose digestion pattern (3 bands- 3571bp, 1164bp and 806bp) is accordance with the theoretical map (D). **(D)** Hypothetical *HindIII* restriction graphs of pICSL01005::cDNA (RPR2) **(E)**Physical gel for *SacI* digestion screen and PCR check of pICSL01005::cDNA (RPR1). The Red arrow has marked out the positive cloning in lane 3 of *SacI* digestion part of gel (left part of gel) whose digestion pattern (2 bands- 3571bp and 2412bp merges together, and 1142bp) is in accordance with the theoretical map (F). That the colony PCR band of lane 3 is identical to the whole length of RPR1 cDNA (3879bp), has verified the digestion screen result. **(F)** Hypothetical *SacI* restriction graphs

of pICSL01005::cDNA (RPR1)

4. Discussion

In this study, we have cloned the whole length gene sequence of CC-NLR pair RPR1 & 2 from *Oryza Sativa Japonica* using the Golden Gate cloning technology. The subcellular localization study using a RPR1 fused to eCFP tag and RPR2 fused to YFP tag revealed nuclear localization pattern for both proteins when transiently expressing in *N. benthamiana* (Fig 3.5). It is clear that RPR1 and RPR2 have shared the same subcellular localization pattern, however, we still don't know whether they could bind with each other to function jointly like the previously reported TIR-NLR pair RRS1 and RPS4 of *Arabidopsis* (Sarris et al., 2015; Le Roux et al., 2015, Sung Un Huh et al., 2017) and the CC-NLR pair RGA4 and RGA5 of rice (Césari et al., 2014). To address this concern, co-immunoprecipitation and BiFC assays could be adopted and applied to investigate the interacting activity of RPR1&2, and the Golden Gate cloning will provide great ease and convenience for preparing constructs with different tags.

The results of confocal microscopy (Fig 3.5) and cDNA cloning (Fig 3.7) both indicate that gene *RPR1* and *RPR2* have been translated and expressed during the agroinfiltration assay. To analyze the functional role of this CC-NLR immune receptor pair, effector AvrRps4 or PopP2 were co-agroinfiltrated with RPR1/RPR2 in *N. tabacum.* HR-like response was observed in PopP2 treatment. We call it HR-like response, since, it differs from the typical HR of transparent and sharp-edged tissue region, the response triggered by PopP2 seems quite weak - with only chlorosis symptoms shown within co-infiltrated region, results are consistent though (Fig 3.6, Figure S5). According to Sarris et al. (Sarris et al., 2015, Ma et al., 2018), PopP2 acetylates RRS1-R and RRS1-S WRKY domains at two Lysines of the canonical WR**K**YGQ**K** sequence, followed by the defense activation. As mentioned in introduction, RPR1 carries 2 WRKY domains, while RRS1 has only one (Fig 3.1) Would two WRKY domains facilitate or pose difficulty for PopP2 recognition? We still don't know.

Apart from PopP2, effector AvrRps4 didn't trigger HR response when co-infiltrated with RPR1&2. Previous study on TIR-NLR pair RRS1/RPS4 suggested that unlike PopP2 which interacts specifically with the WRKY domain and acetylates Lysines within WRKYGQK motif, the interactions between RRS1-WRKY and AvrRps4 are necessary but not sufficient for genetic recognition of AvrRps4, which also interacts with other domains of RRS1 (Sarris et al., 2015).

As suggested in the recently published article (Ma et al., 2018), PopP2 and AvrRPS4 activate NLR RRS1/RPS4 through distinct mode. WRKY domain contributes to maintaining the complex in an inactive state by interacting with the adjacent domain 4 of RRS1. AvrRps4 interaction with the WRKY domain disrupts WRKY-domain 4 association, thus relieving the negative effect of WRKY posed on RRS1 and activating the NLR pair. However, PopP2-triggered activation involves the longer C-terminal extension of RRS1-R. Furthermore, some mutations in RPS4 and RRS1 compromise PopP2 but not AvrRps4 recognition, suggesting that AvrRps4 and PopP2 derepress the WRKY-domain 4 complex differently (Ma et al., 2018).

As we introduced before, the RPS4/RRS1 pair is paired TIR-NLRs (TNLs), whileRPR1&2 area set of hypothetical CC-NLRs (CNLs). The structural differences between TNL RRS1/RPS4 and CNL RPR1/2 might lay the explanation for the experimental results of HR.

Reference

Boller, T., and Felix, G. (2009). A renaissance of elicitors: perception of microbe-associated molecular patterns and danger signals by pattern-recognition receptors. Annual review of plant biology *60*, 379-406.

Bonardi, V., Cherkis, K., Nishimura, M.T., and Dangl, J.L. (2012). A new eye on NLR proteins: focused on clarity or diffused by complexity? Current opinion in immunology *24*, 41-50.

Cesari, S., Bernoux, M., Moncuquet, P., Kroj, T., and Dodds, P.N. (2014). A novel conserved mechanism for plant NLR protein pairs: the "integrated decoy" hypothesis. Frontiers in plant science *5*, 606.

Césari, S., Kanzaki, H., Fujiwara, T., Bernoux, M., Chalvon, V., Kawano, Y., Shimamoto, K., Dodds, P., Terauchi, R., and Kroj, T. (2014). The NB-LRR proteins RGA4 and RGA5 interact functionally and physically to confer disease resistance.

Chavarríasmith, J., and Vance, R.E. (2013). Direct Proteolytic Cleavage of NLRP1B Is Necessary and Sufficient for Inflammasome Activation by Anthrax Lethal Factor.

PLoS pathogens *9*, e1003452.

Chi, Y., Yang, Y., Zhou, Y., Zhou, J., Fan, B., Yu, J.-Q., and Chen, Z. (2013). Protein–protein interactions in the regulation of WRKY transcription factors. Molecular plant *6*, 287-300.

Danot, O., Marquenet, E., Vidalingigliardi, D., and Richet, E. (2009). Wheel of Life, Wheel of Death: A Mechanistic Insight into Signaling by STAND Proteins. Structure *17*, 172-182.

Dodds, P.N., and Rathjen, J.P. (2010). Plant immunity: towards an integrated view of plant-pathogen interactions. Nature reviews Genetics *11*, 539-548.

Duxbury, Z., Ma, Y., Furzer, O.J., Huh, S.U., Cevik, V., Jones, J.D.G., and Sarris, P.F. (2016). Pathogen perception by NLRs in plants and animals: Parallel worlds. Bioessays *Accepted*, 769-781.

Ea, V.D.B., and Jones, J.D. (1998). The NB-ARC domain: a novel signalling motif shared by plant resistance gene products and regulators of cell death in animals. Current biology : CB *8*, R226.

Elinav, Strowig, HenaoMejia, Jorge, Richard, and nbsp (2011). Regulation of the Antimicrobial Response by NLR Proteins. Immunity *34*, 665.

Engler, C., Gruetzner, R., Kandzia, R., and Marillonnet, S. (2009). Golden gate shuffling: a one-pot DNA shuffling method based on type IIs restriction enzymes. PloS one *4*, e5553.

Engler, C., Kandzia, R., and Marillonnet, S. (2008). A one pot, one step, precision cloning method with high throughput capability. PloS one *3*, e3647.

Engler, C., Youles, M., Gruetzner, R., Ehnert, T.-M., Werner, S., Jones, J.D.G., Patron, N.J., and Marillonnet, S. (2014). A golden gate modular cloning toolbox for plants.

ACS synthetic biology *3*, 839-843.

Finger, J.N., Lich, J.D., Dare, L.C., Cook, M.N., Brown, K.K., Duraiswami, C., Bertin, J., and Gough, P.J. (2012). Autolytic proteolysis within the function to find domain (FIIND) is required for NLRP1 inflammasome activity. Journal of Biological Chemistry *287*, 25030-25037.

Gassmann, W., Hinsch, M.E., and Staskawicz, B.J. (1999). The *Arabidopsis* RPS4 bacterial‐resistance gene is a member of the TIR‐NBS‐LRR family of disease‐resistance genes. The Plant Journal *20*, 265-277.

Hu, Z., Yan, C., Liu, P., Huang, Z., Ma, R., Zhang, C., Wang, R., Zhang, Y., Martinon, F., and Miao, D. (2013). Crystal structure of NLRC4 reveals its autoinhibition mechanism. Science *341*, 172-175.

Jacob, F., Vernaldi, S., and Maekawa, T. (2013). Evolution and Conservation of Plant NLR Functions. Frontiers in Immunology *4*, 297.

Jones, J.D.G., and Dangl, J.L. (2006). The plant immune system. Nature *444*, 323-329.

Jones, J.D.G., Vance, R.E., and Dangl, J.L. (2016). Intracellular innate immune surveillance devices in plants and animals. Science *354*, aaf6395.

Koonin, E.V., and Aravind, L. (2000). The NACHT family - a new group of predicted NTPases implicated in apoptosis and MHC transcription activation. Trends in biochemical sciences *25*, 223.

Koonin, E.V., and Aravind, L. (2002). Origin and evolution of eukaryotic apoptosis: the bacterial connection. Cell Death & Differentiation *9*, 394-404.

Kroj, T., Chanclud, E., Michelromiti, C., Grand, X., and Morel, J.B. (2016). Integration of decoy domains derived from protein targets of pathogen effectors into plant

immune receptors is widespread. New Phytologist *210*, 618-626.

Le, R.C., Huet, G., Jauneau, A., Camborde, L., Trémousaygue, D., Kraut, A., Zhou, B., Levaillant, M., Adachi, H., and Yoshioka, H. (2015). A receptor pair with an integrated decoy converts pathogen disabling of transcription factors to immunity. Cell *161*, 1074-1088.

Leipe, D.D., Koonin, E.V., and Aravind, L. (2004). STAND, a Class of P-Loop NTPases Including Animal and Plant Regulators of Programmed Cell Death: Multiple, Complex Domain Architectures, Unusual Phyletic Patterns, and Evolution by Horizontal Gene Transfer. Journal of Molecular Biology *343, 1-28.*

Hao, W., Collier, S. M., Moffett, P., Chai, J. (2013) Structural basis for the interaction between the potato virus X resistance protein (Rx) and its cofactor Ran GTPase-activating protein 2 (RanGAP2). The Journal of biological chemistry 288,NO.50,pp.35868–35876.

Huh, S., Cevik, V., Ding, P., Duxbury, Z., Ma, Y., Tomlinson, L., Sarris, P., and Jones, J.D.G. (2017) Protein-protein interactions in the RPS4/RRS1 immune receptor complex. PLOS Pathogens, 13(5):e1006376

Ma, Y., Guo, H., Hu, L., Martinez, P., Moschou, P., Cevik, V., Ding, P., Duxbury, Z., Sarris, P., and Jones, J.D.G. (2018) Distinct modes of derepression of an Arabidopsis immune receptor complex by two different bacterial effectors. PNAS, www.pnas.org/cgi/doi/10.1073/pnas.1811858115

Mackey, D., Rd, H.B., Wiig, A., and Dangl, J.L. (2002). RIN4 interacts with Pseudomonas syringae type III effector molecules and is required for RPM1-mediated resistance in Arabidopsis. 108, 743–754.

Narusaka, M., Kubo, Y., Hatakeyama, K., Imamura, J., Ezura, H., Nanasato, Y., Tabei, Y., Takano, Y., Shirasu, K., and Narusaka, Y. (2013). Interfamily Transfer of Dual NB-LRR Genes Confers Resistance to Multiple Pathogens. PloS one *8*, e55954.

Ntoukakis, V., Saur, I.M., Conlan, B., and Rathjen, J.P. (2014). The changing of the guard: the Pto/Prf receptor complex of tomato and pathogen recognition. Current opinion in plant biology *20*, 69-74.

Rairdan, G. J., Collier, S. M., Sacco, M. A., Baldwin, T. T., Boettrich, T., Moffett, P. (2008). The Coiled-Coil and Nucleotide Binding Domains of the Potato Rx Disease Resistance Protein Function in Pathogen Recognition and Signaling. The Plant Cell 20: 739–751.

Sarris, P.F., Cevik, V., Dagdas, G., Jones, J.D., and Krasileva, K.V. (2016). Comparative analysis of plant immune receptor architectures uncovers host proteins likely targeted by pathogens. BMC biology *14*, 8.

Sarris, P.F., Duxbury, Z., Huh, S.U., Ma, Y., Segonzac, C., Sklenar, J., Derbyshire, P., Cevik, V., Rallapalli, G., Saucet, S.B.*, et al.* (2015). A Plant Immune Receptor Detects Pathogen Effectors that Target WRKY Transcription Factors. Cell *161*, 1089-1100.

Saucet SB, Ma Y, Sarris PF§, Furzer JO, Sohn KH, and Jones JD. (2015). Two linked pairs of *Arabidopsis* TNL resistance genes function independently to recognize bacterial effector AvrRps4. Nature Comm. Vol 6:6338, doi/10.1038/ncomms7338.

Schreiber, K.J., Bentham, A., Williams, S.J., Kobe, B., and Staskawicz, B.J. (2016). Multiple Domain Associations within the *Arabidopsis* Immune Receptor RPP1 Regulate the Activation of Programmed Cell Death. PLoS pathogens *12*, e1005769.

Tasset, C., Bernoux, M., Jauneau, A., Pouzet, C., Brière, C., Kieffer-Jacquinod, S., Rivas, S., Marco, Y., and Deslandes, L. (2010). Autoacetylation of the Ralstonia solanacearum effector PopP2 targets a lysine residue essential for RRS1-R-mediated immunity in *Arabidopsis*. PLoS pathogens *6*, e1001202.

Weber, E., Engler, C., Gruetzner, R., Werner, S., and Marillonnet, S. (2011). A modular cloning system for standardized assembly of multigene constructs. PloS

one *6*, e16765.

Williams, S.J., Sohn, K.H., Wan, L., Bernoux, M., Sarris, P.F., Segonzac, C., Ve, T., Ma, Y., Saucet, S.B., and Ericsson, D.J. (2014). Structural Basis for Assembly and Function of a Heterodimeric Plant Immune Receptor. Science *344*, 299.

Yue, J.X., Meyers, B.C., Chen, J.Q., Tian, D., and Yang, S. (2012). Tracing the origin and evolutionary history of plant nucleotide-binding site–leucine-rich repeat (NBS-LRR) genes. New Phytologist *193*, 1049-1063.

Supplemental information

Supplemental 1

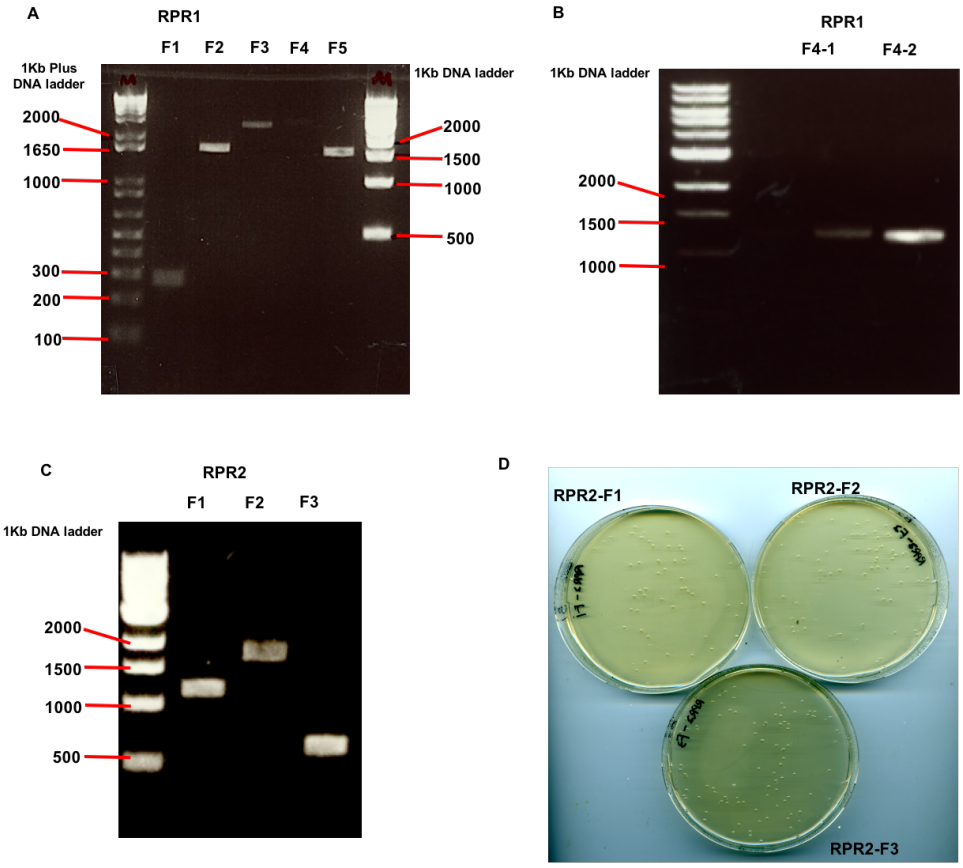

Figure Supplemental 1. **DNA fragment amplification and T-A cloning. (A)** From left to right shows the PCR amplification result of RPR1- Fragment 1, 2, 3, 5， with the band size 253bp for RPR1- Fragment 1, 1527bp for Fragment 2, 2330bp for fragment 3, and 1438bp for fragment 5 **(B)** From left to right shows the PCR amplification result of RPR1- Fragment 4-1 and 4-2, with the band size 1228bp for RPR1- Fragment 4-1, 1280bp for Fragment 4-2. **(C)** From left to right shows the PCR amplification result of RPR2- Fragment 1, 2, 3, with the band size 1163bp for RPR2- Fragment 1, 1770bp for Fragment 2, 608bp for fragment 3. **(D)** The three Petri dishes shows the transformation after T-A cloning of RPR2- Fragment1,2,3.

Supplemental 2

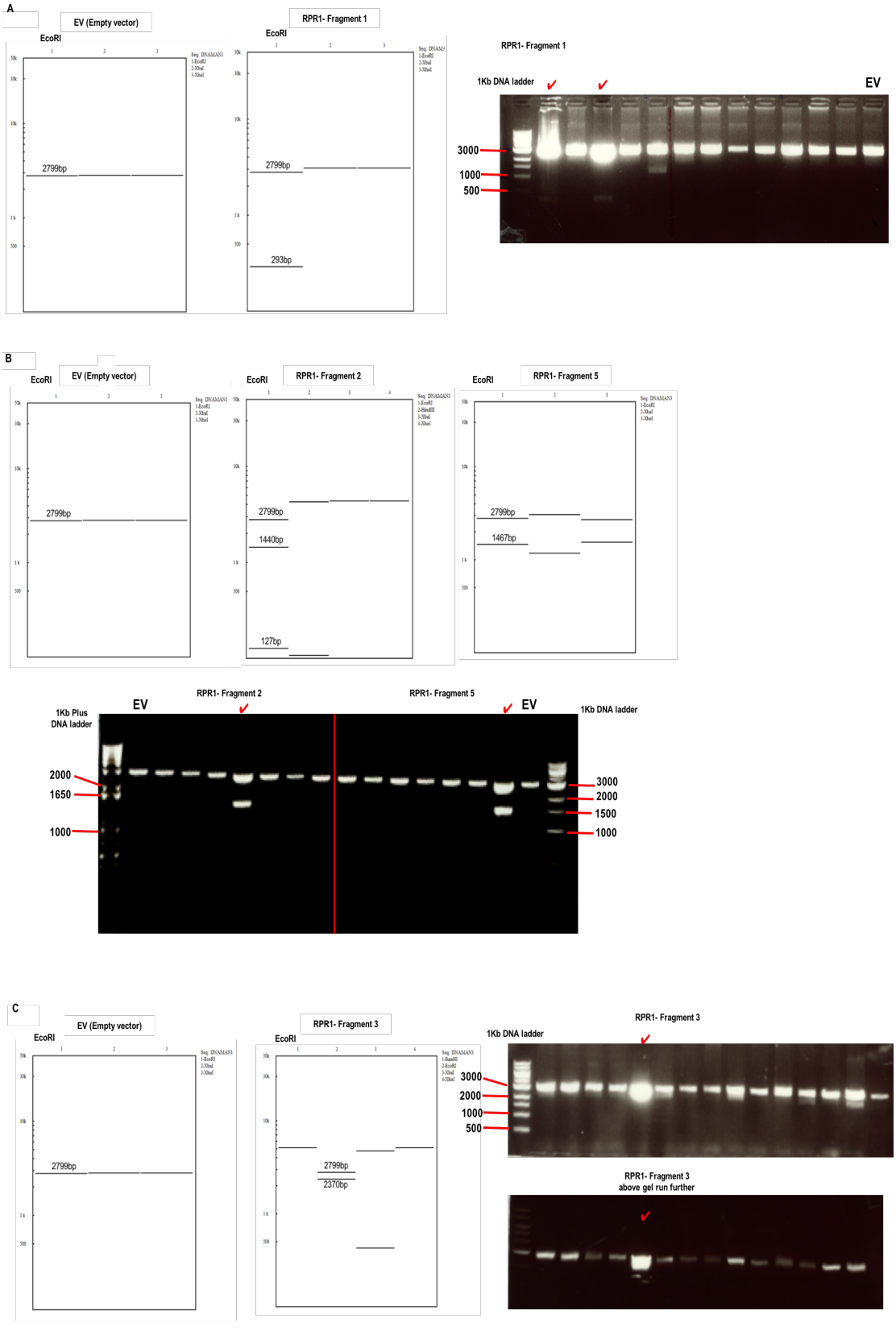

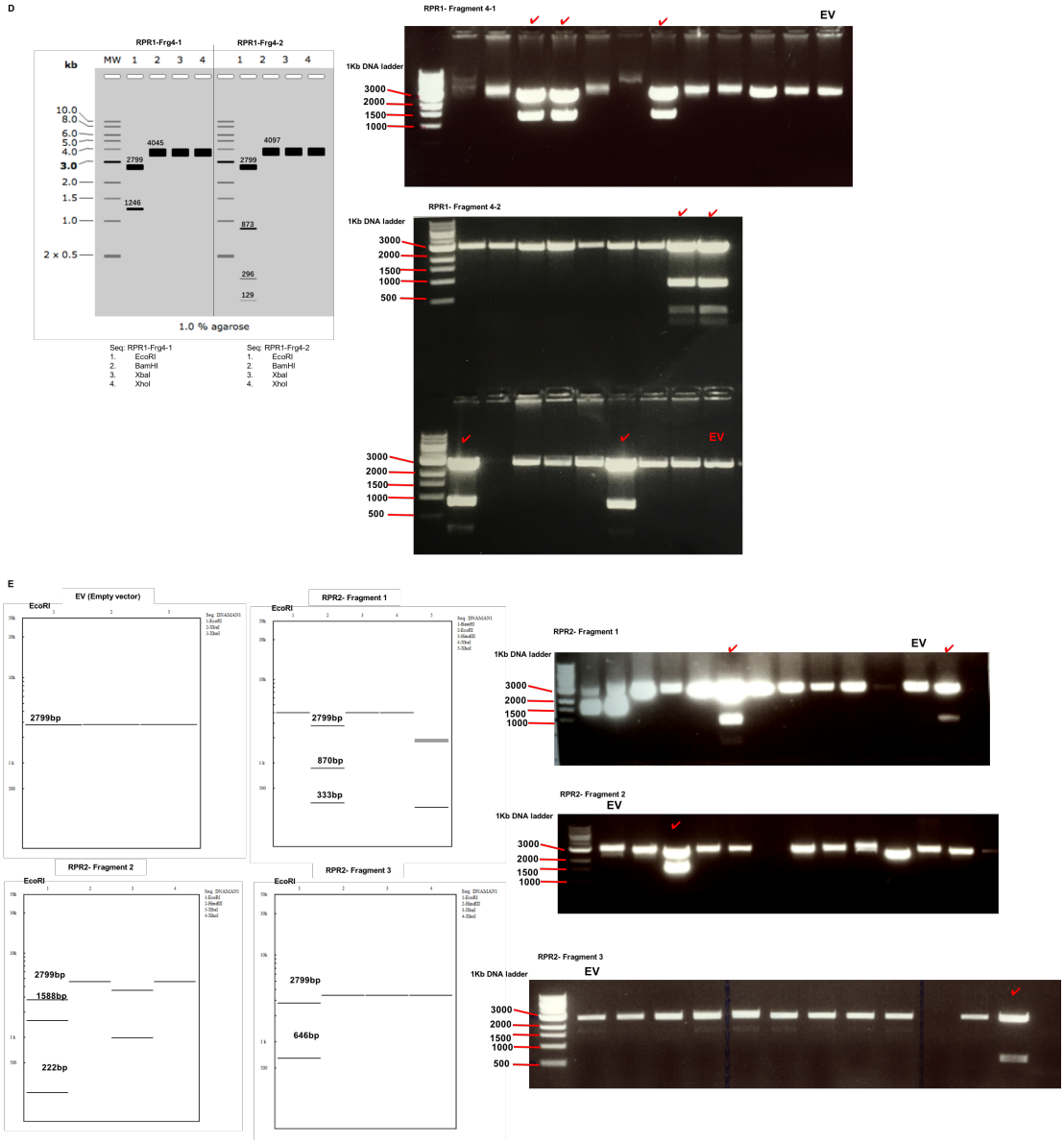

Figure Supplemental 2. **T-A cloning screen through enzyme digestion. (A)** Screen for RPR1-Fragment 1. The two hypothesis digestion maps one the left are *EcoRI* digestion maps for pCRTM8/GW/TOPO empty vector and pCRTM8/GW/TOPO-RPR1-fragment 1 integrated vector, respectively, with only one band (2799bp) for empty vector and two bands (2799bp and 293bp) for the T vector integrated with RPR1-fragment 1. The physical nucleic gel on the right showed the digestion results, with the red arrow marked the positive cloning, of which digestion pattern was in accordance with hypothesis digestion on the left. **(B)** Screen for RPR1-Fragment 2 and 5. Similar to (A) , it exhibited hypothesis digestion maps of pCRTM8/GW/TOPO empty vector, and pCRTM8/GW/TOPO-RPR1-fragment 2, -fragment 5 integrated vector, respectively. Positive closings were found in accordance with theoretical digestion patterns and marked with red in the physical gel at the bottom. **(C)** Screen for RPR1-Fragment 3. The two hypothesis digestion maps on the left exhibited hypothesis digestion maps of pCRTM8/GW/TOPO empty vector, and pCRTM8/GW/TOPO-RPR1-fragment 3 integrated vector, respectively. The two physical gels on the right were the same gels, but with the bottom one ran longer electrophoresis time and took shorter exposure time. The red arrow marked on the gels indicates the positive cloning with two bands (2799bp and 2370bp). **(D)** The

left picture shows the hypothesis digestion maps of pCRTM8/GW/TOPO-RPR1-fragment 4-1 and 4-2, whose physical gels are on the right hand side with RPR1-fragment 4-1 on the top and fragment 4-2 at the bottom. **(E)** The four theoretical maps on the left exhibit the hypothesis digestion patterns of pCRTM8/GW/TOPO-RPR1 empty vector, pCRTM8/GW/TOPO- RPR2-Fragment 1, 2 and 3 integrated vectors, respectively. Physical gels on the right hand side, from top to the bottom, show the digestion result of RPR2-Fragment 1, 2 and 3.

Supplemental 3

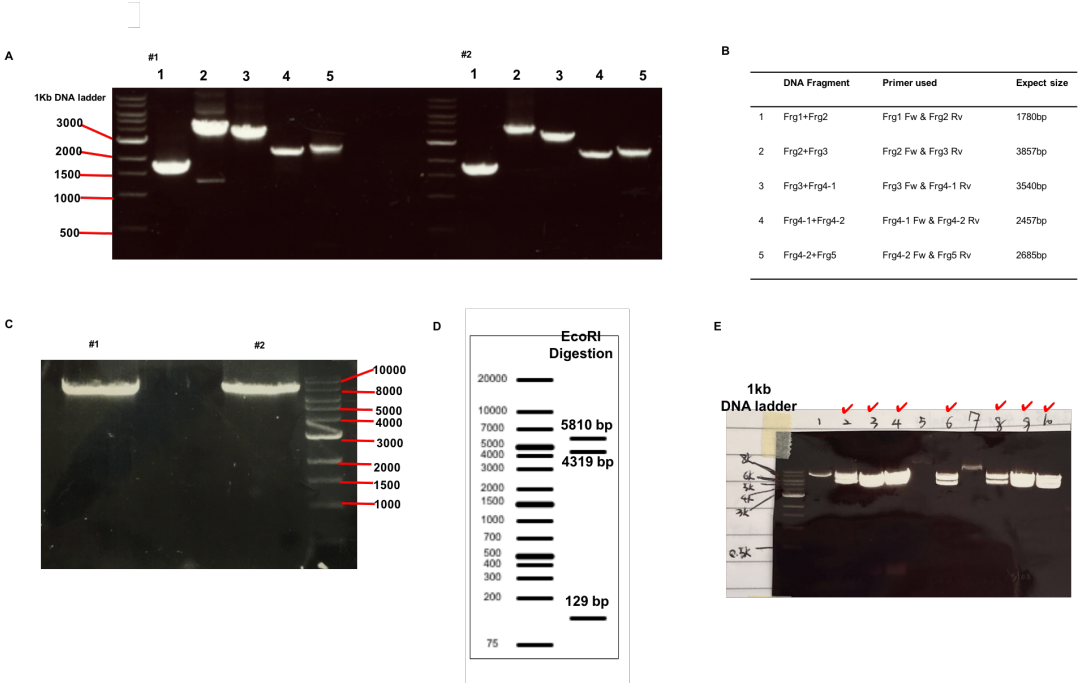

	DNA Fragment	Primer used	Expect size
1	Frg1+Frg2	Frg1 Fw & Frg2 Rv	1780bp
2	Frg2+Frg3	Frg2 Fw & Frg3 Rv	3857bp
3	Frg3+Frg4-1	Frg3 Fw & Frg4-1 Rv	3540bp
4	Frg4-1+Frg4-2	Frg4-1 Fw & Frg4-2 Rv	2457bp
5	Frg4-2+Frg5	Frg4-2 Fw & Frg5 Rv	2685bp

Figure Supplemental 3. **Validity check of pICSL86922::RPR1-eCFP. (A)** Fragment PCR for screened pICSL86922::RPR1-eCFP. Two screened colonings, #1 and #2, are used for fragment PCR to double check the result. From lane 1 to 5, fragment combination, band size and primers are in accordance with (B). **(B)** Primers used and band sized expected for fragment PCR of pICSL86922::RPR1-eCFP. **(C)** Whole length PCR of pICSL86922::RPR1-eCFP. The whole length of RPR1 genomic DNA is amplified by using #1 and #2 construct DNA as template **(D)** Hypothetical *EcoRI* restriction graphs of pICSL86922::RPR1-eCFP. Three bands 5810bp, 4319bp and 129 bp appears in the map. **(E)** Physical gel for *EcoRI* digestion screen of pICSL86922::RPR1-eCFP. Red arrow has marked out the positive colonings which mains the digestion pattern similar to (D).

Supplemental 4

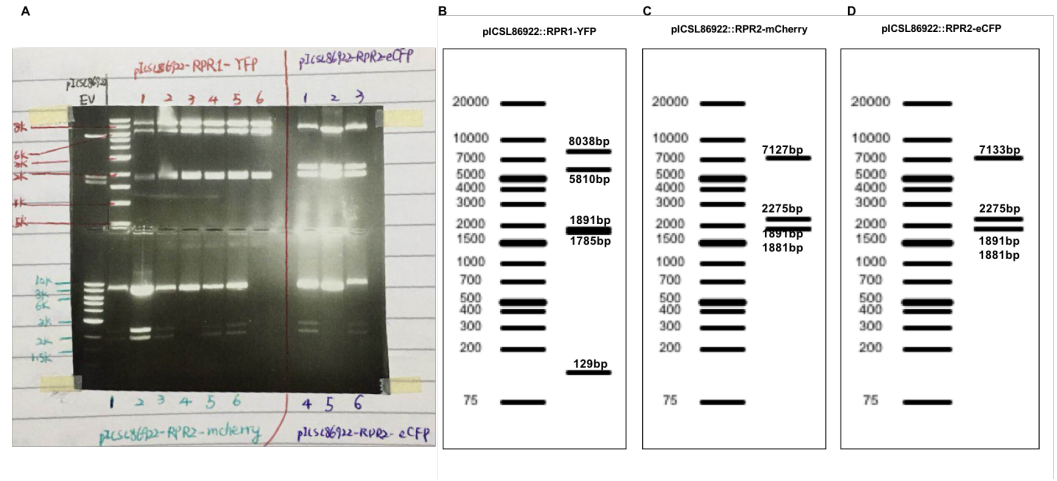

Figure Supplemental 4. **Making constructs of pICSL86922. (A)** Physical gel for constructs screen of pICSL86922::RPR1-YFP, pICSL86922::RPR2-eCFP, pICSL86922::RPR2-mCherry, and pICSL86922::RPR2-eCFP. All the samples subjected to digestion are positive clonings. EV stands for empty vector digestion. **(B)** Hypothetical *EcoRI* restriction graphs of pICSL86922::RPR1-YFP. **(C)** Hypothetical *EcoRI* restriction graphs of pICSL86922::RPR2-mCherry. **(D)** Hypothetical *EcoRI* restriction graphs of pICSL86922::RPR2-eCFP.

Supplemental 5

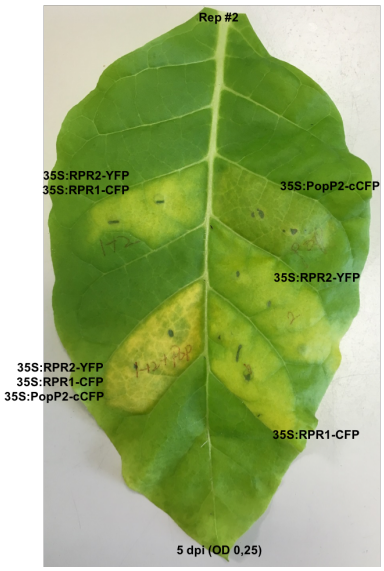

Figure Supplemental 5. **HR test of paired cc-NLR RPR1&2 with effector PopP2.** Compared with Figure 8, Supplemental 3 is used the same treatment for agroinfiltration assays in N. tabacum, but used older leaves. As previously described, five treatments were carried out within one leaf: infiltrate with RPR1 only, RPR2 only, PopP2 only, co-infiltrate with RPR1/RPR2 pair, and co-infiltrate with

effector PopP2 and RPR1/RPR2 pair. The PopP2 and RPR1/RPR2 co-infiltration area shows more serious yellow lesion symptoms than other injected leaf areas.